structural interpretation of the shifts inasmuch as structural and bonding changes are expected to have similar effects on each of the dioxygen isotopomers of a given protein. In fact, for one of the protein systems studied, the shift for one isotopic ν(O–O) is 9 cm^{-1} different from that for another isotopomer (i.e., $\nu(^{18}O–^{18}O)$ and $\nu(^{16}O–^{18}O)$ of the β subunit, Figure 4).

As is clear from the discussion in previous sections of this work, H_2O/D_2O exchange (which leads to NH/ND exchange of the histidyl imidazole fragments) may differentially alter the vibrational interaction between the various isotopomer ν(O–O)'s and the imidazole modes, thus giving rise to a wide variation in observed H_2O/D_2O shifts. To the extent that such shifts cannot then be ascribed to changes in hydrogen bond strength, they cannot be taken as evidence for distal side hydrogen bonding.

We wish to emphasize that the present interpretation does not imply that distal side hydrogen bonding is nonexistent but simply that the observed H_2O/D_2O shifts are the result of altered vibrational coupling patterns rather than altered hydrogen bond strengths. In fact, the ν(O–O) frequencies observed for the proteins and the model compounds are consistent with the distal side hydrogen bonding proposal. Thus, the proteins exhibit $\nu(^{16}O–^{16}O)$ and $\nu(^{18}O–^{18}O)$ at $\sim$1135 and $\sim$1065 cm^{-1}, respectively. The corresponding values for various (non-hydrogen bonded) models are $\sim$1145 and $\sim$1075 cm^{-1} (Figure 8 and ref 16–18). As our earlier model compound study had shown,[17] shifts of this magnitude ($\sim$10 cm^{-1}) may reasonably be ascribed to hydrogen bonding to the distal histidylimidazole.

Conclusions

The general vibrational patterns and appearance of multiple oxygen-sensitive bands in the RR spectra of oxygenated cobalt-substituted heme proteins can be rationalized by the proposal that the bound dioxygen is vibrationally coupled to internal modes of the proximal or distal histidylimidazole. The effects of such coupling can generally be demonstrated with model compound studies, to the extent that reliable models can be devised (i.e., certain subtle structural features of the protein are difficult to duplicate). This interpretation provides plausible explanations for observed D_2O and oxygen isotopomer shifts as well as the appearance of weak secondary bands without requiring the existence of two liganded structures and, in fact, would indicate that if two such conformers do exist in solution, they exhibit similar values of ν(O–O).

Finally, while the apparent vibrational coupling of bound dioxygen with internal modes of histidylimidazole complicates the spectral interpretation, it is interesting to consider the potential utility of such measurements. Thus, rather than representing an experimental nuisance, it offers promise as a spectroscopic probe of internal modes of histidine and its interaction with the heme. For example, if the observed intensity of the feature located at 1150 cm^{-1} is indeed correlated with the proximal histidyl plane-orientation angle as the comparison of the limited data might suggest, it would serve as a relatively convenient probe of this possibly important[34] structural parameter. In addition to studies of static systems, useful experiments involving spectroscopic transients are conceivable. Further documentation of this effect and determination of the factors which lead to effective coupling will require the study of more sophisticated model compounds as well as modified and mutant hemoglobins. Such studies are currently underway in our laboratory, and several time-resolved RR studies to probe spectroscopic transients are planned.

Acknowledgment. We gratefully acknowledge support of this work from the National Institutes of Health (DK 35153) and the National Science Foundation (CHE-8413956).

Registry No. 4-MI, 822-36-6; 4-MI-$^2H_1$, 2519-73-5; 4-MI-d_3, 115482-88-7; 4-MI-d_2, 115482-89-8; PP, 553-12-8; CoPP, 14325-03-2; CH_3O^2H, 1455-13-6; NaO^3H, 14014-06-3; cobaltous acetate, 71-48-7.

Crystal Structure, CP/MAS ^{129}Xe, and ^{13}C NMR of Local Ordering in Dianin's Compound Clathrates†

F. Lee, E. Gabe, J. S. Tse, and J. A. Ripmeester*

Contribution from the Division of Chemistry, National Research Council of Canada, Ottawa, Ontario K1A 0R9, Canada. *Received December 9, 1987*

Abstract: The ^{129}Xe and ^{13}C CP/MAS NMR spectra of xenon-containing clathrates of Dianin's compound (4-*p*-hydroxyphenyl-2,2,4-trimethylchroman) are more complicated than expected for fully ordered materials. Single-crystal X-ray diffraction was used to show that there is a single site for xenon in the structure, the only variable being the site occupancy. The NMR spectra therefore were interpreted in terms of small differences in local order. The NMR spectrum of trapped xenon is sensitive to the absence or presence of a second guest in the double cage and in some instances also is sensitive to the nature of this guest as well as the guests in adjoining cages. There is no evidence for preferential formation of Xe dimers in the cages. NMR spectroscopy allows a description of the clathrate which is largely complementary to the structural data from X-ray diffraction.

In recent years, ^{129}Xe NMR, due to the great sensitivity of the Xe nuclear shielding to the Xe atom's physical surroundings, has become an important tool in the study of a variety of phenomena. These include the study of site occupancies in clathrate hydrates,[1,2] other inclusion compounds,[3] and zeolites[4-8] as well as the probing of solution structure[9-12] including hydrophobic interactions in protein and micellar solutions.

Recently two approaches[13,14] have been suggested to account for ^{129}Xe NMR shifts in zeolites. One approach correlates the ^{129}Xe shift with mean free path,[13] the other with surface curvature.[14] However, neither of these can be used to explain the anisotropic chemical shifts observed in solid-like environments.[3] Once a detailed understanding of ^{129}Xe shielding is obtained there

† NRCC no. 28802.

(1) Ripmeester, J. A.; Davidson, D. W. *Bull. Magn. Reson.* **1980**, *2*, 139.
(2) Davidson, D. W.; Handa, Y. P.; Ripmeester, J. A. *J. Phys. Chem.* **1986**, *90*, 6549.
(3) Ripmeester, J. A. *J. Am. Chem. Soc.* **1982**, *104*, 209.
(4) Ito, T.; Fraissard, J. *Proceedings of the 5th Conference on Zeolites*; Heyden: London, 1981; p 510.
(5) de Menorval, L. D.; Fraissard, J. P. *J. Chem. Soc., Faraday Trans. 1* **1982**, *78*, 403.
(6) Ripmeester, J. A. *J. Magn. Reson.* **1984**, *56*, 247.
(7) Ito, T.; Fraissard, J. *J. Chem. Phys.* **1982**, *76*, 5225.
(8) Ito, T.; de Menorval, L. C.; Guerrirer, E.; Fraissard, J. *Chem. Phys. Lett.* **1984**, *111*, 271.

0002-7863/88/1510-6014$01.50/0 Published 1988 by the American Chemical Society

is some hope that ^{129}Xe NMR can be used to study void spaces in systems of low order such as glasses and other amorphous materials.

A class of materials which can be put to use in investigating ^{129}Xe shielding effects is that of clathrates and inclusion compounds, as often long range crystalline order can exist alongside local disorder (e.g., vacant sites or site occupancy by different guests). A detailed investigation of nuclear shielding correlations with structure in materials such as clathrate hydrates and clathrasils is hampered by the fact that their compositions cover only a limited range and the difficulty of sample preparation. However there are good empirical correlations of cage free space with the isotropic nuclear shielding and of cage shape with nuclear shielding anisotropy.[1-3]

Dianin's compound clathrates offer an attractive possibility of studying factors affecting nuclear shielding. With many guest species Dianin's compound forms well-ordered, crystalline clathrates.[15,16] Six phenolic hydroxyls form hydrogen-bonded hexagonal rings with alternate host molecules pointing in opposite directions out of the ring plane. Stacks of such units form hour-glass shaped cages with two wide sections of some 6.3 Å radius free space joined by a narrower neck. Small guests occupy the wide cage portions, two to a cage, whereas larger guests make use of both the wide portions as well as the neck. The lattice has sufficient flexibility to accommodate guests of widely different sizes and shapes.[15] Therefore, with mixed guest species it may be expected that although the host lattice maintains long-range order, there may well be some short-range disorder depending on the exact distribution of the guest molecules or on the presence of empty cages.

One study[17] on the Xe clathrate of Dianin's compound is available, a low-temperature study of Xe sorption by Dianin's compound under grinding action. The volume of gas sorbed required the presence of as many as 3.3 Xe atoms per cage.

The initial problem, therefore, was to see if Xe NMR could be used to identify different sites for Xe in the lattice. As the ^{129}Xe NMR spectrum did not prove simple to assign, a number of samples of different compositions were studied by ^{129}Xe as well as ^{13}C NMR. In addition, the crystal structure of the xenon clathrate of Dianin's compound was solved by means of X-ray diffraction. Most of the features of the ^{129}Xe NMR spectrum then could be explained in terms of local ordering. In addition, more features of ^{13}C NMR spectrum of the flexible host lattice could be explained in light of this new information.

Experimental Section

NMR Experiments. ^{13}C and ^{129}Xe NMR spectra were obtained at frequencies of 45.28 and 49.8 MHz on a Bruker CXP-180 NMR spectrometer equipped with a Doty Scientific probe. Single cross-polarization contacts[18] of 5–20-ms duration were used with matched rf amplitudes of 75 kHz. Decays of 2–3 K datum points were collected at a sweep width setting of 20 kHz with a delay time of 2 s. Magic angle spinning[19] rates of ~4 kHz were employed, in some cases with first-order side band suppression.[20] ^{129}Xe NMR shifts are reported with respect to gas at zero density. In practice a xenon–quinol sample was used as a secondary standard.

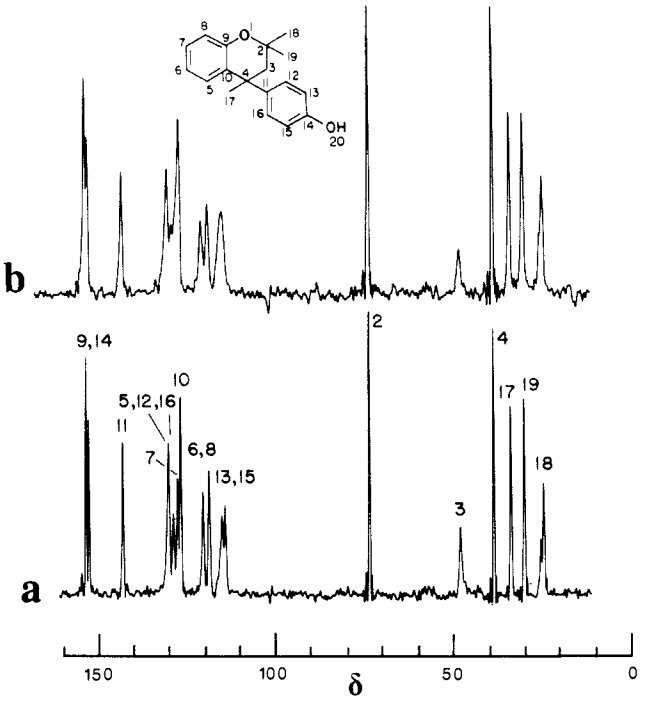

Figure 1. ^{13}C CP/MAS NMR spectra of Dianin's compound clathrates of xenon (a) sample prepared from *m*-xylene solution and (b) sample prepared by low-temperature grinding. First-order spinning sidebands were suppressed.

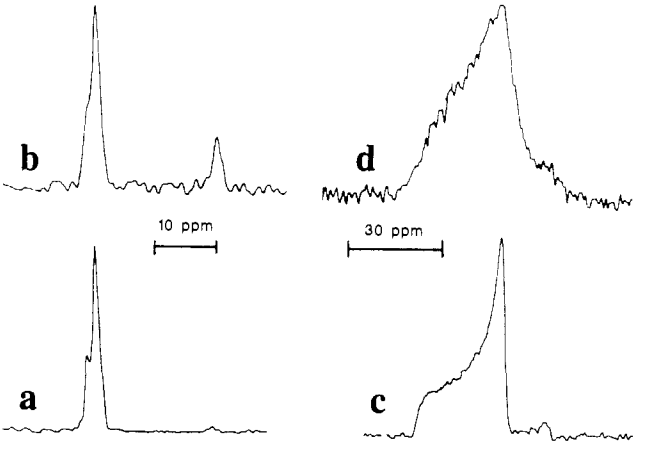

Figure 2. ^{129}Xe CP NMR spectra of Dianin's compound clathrates (a,b) with magic angle spinning for samples prepared from *m*-xylene and by low-temperature grinding, respectively; (c,d) as for (a,b) nonspinning samples.

X-ray Diffraction. Diffraction intensities were collected with graphite monochromatized Cu Kα radiation with the $\theta/2\theta$ scan technique with profile analysis to $2\theta_{max} = 120°$. The 0.23 × 0.3 × 0.3 mm crystal was grown from *m*-xylene under ~1 atm xenon pressure. A total of 2956 reflections were measured of which 2350 were unique, and 1758 reflections were considered significant with $I_{net} > 2.5\sigma(I_{net})$. Lorentz and polarization factors were applied, but no absorption corrections were made ($\mu = 4.7$ mm^{-1}). The cell parameters were obtained by least-squares refinement of the setting angles of 70 reflections with $2\theta > 100°$ ($\lambda_{Cu\ K\alpha 1} = 1.5406$ Å). All calculations were performed with the NRC VAX system of computer programs. Scattering factors were taken from *International Tables for X-ray Crystallography*.

Sample Preparation. Dianin's compound (4-*p*-hydroxyphenyl-2,2,4-trimethylchroman) was prepared and purified according to literature methods.[15] Samples with low xenon content were prepared by recrystallizing guest-free Dianin's compound from *m*-xylene, dodecane, octane, or ethanol under a low pressure of xenon on a vacuum line. Samples with higher xenon content were prepared by recrystallizing guest-free Dianin's compound from the above solvents under pressures of up to 20 atm of xenon in a Parr pressure vessel.

In order to simulate earlier gas uptake experiments,[17] one sample was prepared by grinding guest-free Dianin's compound under ~5 atm of

(9) Miller, K. W.; Reo, N. V.; Schoot Uiterkamp, A. J. M.; Stengle, D. P.; Stengle, T. R.; Williamson, K. L. *Proc. Natl. Acad. Sci. U.S.A.* **1981**, *78*, 4946.
(10) Tilton, R. F.; Kuntz, I. D., Jr. *Biochemistry* **1982**, *21*, 6851.
(11) Stengle, T. R.; Hosseini, S. M.; Basini, H. G.; Williamson, K. L. *J. Soln. Chem.* **1984**, *13*, 779.
(12) Stengle, T. R.; Williamson, K. L. *Macromolecules* **1987**, *20*, 1428.
(13) Demarquay, J.; Fraissard, J. *Chem. Phys. Lett.* **1987**, *136*, 314.
(14) Derouane, E. G.; Nagy, J. B. *Chem. Phys. Lett.* **1987**, *137*, 341.
(15) Baker, W.; Floyd, A. J.; McOmie, J. W. R.; Pope, G.; Weaving, A. S.; Wild, J. H. *J. Chem. Soc.* **1956**, 2010.
(16) MacNicol, D. D.; McKendrick, J. J.; Wilson, D. R. *Chem. Soc. Rev.* **1978**, *7*, 65.
(17) Barrer, R. M.; Shanson, V. H. *J. Chem. Soc., Chem. Commun.* **1976**, 333.
(18) Pines, A.; Gibby, M. C.; Waugh, J. S. *J. Chem. Phys.* **1973**, *59*, 569.
(19) Schaefer, J.; Chin, S. H.; Weissman, S. I. *Macromolecules* **1972**, *5*, 798.
(20) Hemminga, M. A.; de Jager, P. A. *J. Magn. Reson* **1983**, *52*, 339.

xenon in a Parr pressure vessel, placed in a freezer at −40 °C.

Results and Discussion

Initial Studies. Figures 1 and 2 show ^{129}Xe and ^{13}C CP/MAS NMR spectra of two different samples of Dianin's compound clathrates of xenon. The ^{13}C line assignment was previously[21,22] determined by using dipolar dephasing[23] in combination with ^{2}H substitution at specific carbons.[22]

The ^{13}C NMR spectrum of the sample prepared by low-temperature grinding is considerably less well resolved than the spectrum of the solution grown crystals. For both spectra it is evident that the C_{18} carbon line is split, indicating that there are both filled and empty half-cages. For the spectrum in Figure 1a one of the $C_{13,15}$ lines also has some fine structure.

The ^{129}Xe CP/MAS NMR spectra (Figure 2 (parts a and b)) show two lines some 18 ppm apart with evidence for some fine structure on the low field line.

The lines occur at −152 and −134 ppm, downfield from the gas at zero density. This compared with xenon shifts of −242 and −152 ppm for the small and large cages of the type I xenon hdyrate and −210 ppm for xenon in the β-quinol clathrate cage.[27] The inverse dependence of downfield shift with cage size established previously suggests quite a loose fit for xenon in Dianin's compound.

It is of interest to examine some of the spin dynamics of the trapped xenon, as these properties determine to a large extent the ease with which such a nucleus may be observed. In recording all of the spectra reported here, ^{1}H–^{129}Xe cross-polarization was used to enhance the ^{129}Xe signal, although it turns out that the long ^{129}Xe relaxation time is the main obstacle to efficient observation. Line intensities obtained under cross-polarization conditions must be examined as a function of cross-polarization time in order to establish where reliable equilibrium intensity values can be achieved. The exponential growth constants were ca. 3 ms, so that with a cross-polarization time of ca. 15 ms reliable intensities can be obtained. Evidently there are no slow motions to cause a fast decay of ^{129}Xe line intensity.

The ^{129}Xe spin–lattice relaxation time for the main xenon site in the clathrate was measured to be 300 s. This emphasizes the importance of the cross-polarization technique in short circuiting the slow ^{129}Xe relaxation and avoiding the 10–15-min delay time necessary in any direct observation experiment on xenon.

Figures 2 (parts c and d) show ^{129}Xe NMR spectra for static samples and correspond to spectra shown in Figure 2 (parts a and b) for spinning samples. The well-resolved powder pattern in Figure 2c is characteristic of two axially symmetric shielding tensors with the low-field edges of the patterns coincident. The anisotropic chemical shifts are −54 and −84 ppm, with shielding along the symmetry axis less than that at right angles to the symmetry axis. The other pattern, obtained for the ground sample, is only poorly resolved and indicates that the sample is much less well ordered than the solution sample. However, it is clear that the two samples have xenon atoms distributed in much the same way, even though the assignment is not clear. Therefore it was decided to determine the structure of a solution-grown crystal in the hope that the information gained might lead to an assignment of the ^{129}Xe NMR spectrum.

X-ray Diffraction. The atomic parameters for Dianin's compound in ref 24 were used as the starting point for structural refinement. However, the structure failed to refine. By using a direct method, the structure was solved. It was found that a shift of $^{4}/_{3} - x$, $y - 3 + {}^{2}/_{3}$, $^{2}/_{3} - z$ was required to convert the present coordinate system into one comparable to that in ref 24. The reflection indices were transformed accordingly. This implies a setting ambiguity, as outlined previously for the present space group, which can be resolved by defining the relative magnitudes of pairs of structure factors which are related by ambiguity. There is a further problem associated with this family of clathrates caused by the presence of variable guest molecule occupancy. However, the xenon atom is near the position 0, 0, $^{1}/_{4}$ and so reflections with l odd and small will have small xenon contributions and are therefore suitable to resolve the ambiguity whatever the nature of the guest molecule. Reflections which satisfy both criteria are given in Table I. They help to resolve the ambiguity in terms of the cage atoms alone.

Most of the hydrogen atom positions were calculated, except six of the methyl hydrogen atom positions which were located from a difference map. The structure was refined (hydrogen atom positions fixed) by full-matrix least-squares methods to final residuals of R_f 0.066 and R_w 0.069 for the significant data (R_f 0.086 and R_w 0.077 for all data) with unit weights. The final positional parameters and equivalent isotropic temperature factors are listed in Table II. The distance and angles of the host fragment are listed in Table III. Anisotropic thermal parameters

Table I. Reflections Used To Solve the Setting Ambiguity

h	k	l	F_o	h	k	l	F_o
−4	3	−1	10.3	−3	4	−1	428.0
−4	6	1	126.6	−6	4	−1	333.9
−4	9	1	24.5	−9	4	−1	224.9

Table II. Atomic and Isotropic Thermal Parameters for the Xenon Clathrate of Dianin's Compound

	x	y	z	B_{iso}[a]
Xe	0.00000	0.00000	0.28498 (22)	14.11 (15)
O20	0.06372 (15)	0.11812 (15)	0.9800 (3)	4.24 (20)
O1	0.08659 (20)	0.26053 (20)	0.3743 (3)	4.06 (20)
C14	0.08729 (20)	0.15980 (4)	0.8910 (4)	3.09 (25)
C13	0.13900 (21)	0.17375 (21)	0.8356 (4)	3.4 (3)
C12	0.16808 (22)	0.21465 (21)	0.7448 (4)	3.2 (3)
C11	0.13242 (19)	0.24315 (19)	0.7041 (4)	2.73 (23)
C16	0.08098 (20)	0.22878 (20)	0.7639 (4)	3.1 (3)
C15	0.05906 (20)	0.18828 (21)	0.8551 (4)	3.3 (3)
C14	0.15714 (18)	0.28623 (19)	0.5996 (4)	2.86 (24)
C3	0.64464 (19)	0.25951 (20)	0.4814 (4)	3.1 (3)
C2	0.11055 (21)	0.22405 (21)	0.4071 (4)	3.4 (3)
C9	0.08713 (20)	0.29697 (20)	0.4620 (5)	3.3 (3)
C4	0.11980 (19)	0.31226 (20)	0.5690 (5)	2.98 (25)
C5	0.11760 (22)	0.35242 (21)	0.6460 (5)	3.7 (3)
C6	0.08452 (23)	0.37707 (22)	0.6183 (5)	4.0 (3)
C7	0.05226 (22)	0.36100 (22)	0.5119 (5)	4.1 (3)
C8	0.05381 (21)	0.32226 (22)	0.4326 (5)	3.8 (3)
C19	0.06440 (22)	0.17152 (23)	0.4715 (5)	4.3 (3)
C18	0.12553 (24)	0.2083 (3)	0.2852 (5)	4.7 (3)
C17	0.21762 (24)	0.33496 (21)	0.6369 (5)	3.8 (3)
H13	0.162	0.152	0.864	4.4
H12	0.201	0.225	0.703	4.2
H16	0.059	0.251	0.740	3.9
H15	0.019	0.178	0.899	3.7
H3a	0.195	0.294	0.424	3.8
H36	0.183	0.233	0.536	3.8
H5	0.142	0.365	0.732	4.4
H6	0.083	0.409	0.681	5.1
H7	0.026	0.380	0.492	5.2
H8	0.030	0.312	0.347	4.7
H19a	0.301	0.146	0.415	4.7
H19b	0.047	0.187	0.542	4.7
H19c	0.087	0.150	0.512	4.4
H18a	0.146	0.182	0.301	4.7
H18b	0.151	0.238	0.228	4.7
H18c	0.080	0.180	0.242	5.6
H17a	0.238	0.359	0.566	4.7
H17b	0.222	0.364	0.717	4.7
H17c	0.239	0.311	3.665	3.9

[a] B_{iso} is the mean of the principal axis of the thermal ellipsoid.

(21) Ripmeester, J. A. *J. Inclusion Phenom.* **1983**, *1*, 87.
(22) Barker, P.; Burlinson, N. E.; Dunell, B. A.; Ripmeester, J. A. *J. Magn. Reson.* **1984**, *60*, 486.
(23) Opella, S. J.; Frey, M. H. *J. Am. Chem. Soc.* **1979**, *101*, 5854.
(24) Flippen, J. L.; Karle, J.; Karle, I. L. *J. Am. Chem. Soc.* **1970**, *92*, 3749.
(25) Flippen, J. L.; Karle, J. *J. Phys. Chem.* **1971**, *75*, 3566.
(26) Breitmaier, E.; Voelter, W. *^{13}C NMR Spectroscopy*; Verlag Chemie: Weisheim, New York, 1978.
(27) Davidson, D. W.; Ripmeester, J. A. In *Inclusion Compounds*; Atwood, J., MacNicol, D. D., Davies, J. E. D., Eds.; Academic Press: London, 1984; Vol. 3, p 78.

Table III. Distance (Å) and Angles (deg) for the Xenon Clathrate of Dianin's Compound[a]

	distance		angle
O(20)–C(14)	1.379	O(20)–C(14)–C(13)	121.3
O(1)–C(2)	1.469	O(20)–C(14)–C(15)	119.7
O(1)–C(9)	1.369	C(13)–C(14)–C(15)	119.0
C(14)–C(15)	1.391	C(12)–C(113–C(14)	119.9
C(14)–C(15)	1.384	C(11)–C(12)–C(14)	122.4
C(13)–C(12)	1.379	C(12)–C(11)–C(16)	116.0
C(12)–C(11)	1.404	C(4)–C(11)–C(12)	120.3
C(20)–C(14)	1.404	C(4)–C(11)–C(16)	123.7
C(11)–C(4)	1.526	C(11)–C(16)–C(15)	122.0
C(15)–C(16)	1.376	C(15)–C(16)–C(14)	120.6
C(7)–C(4)	1.540	C(11)–C(4)–C(3)	112.3
C(4)–C(10)	1.528	C(11)–C(4)–C(10)	112.1
C(4)–C(17)	1.556	C(11)–C(4)–C(17)	108.9
C(8)–C(3)	1.518	C(3)–C(4)–C(10)	107.6
C(2)–C(19)	1.515	C(3)–C(4)–C(17)	106.8
C(2)–C(18)	1.513	C(10)–C(4)–C(17)	108.9
C(9)–C(10)	1.398	C(4)–C(3)–C(2)	115.9
C(8)–C(9)	1.413	O(1)–C(2)–C(3)	108.2
C(5)–C(10)	1.398	O(1)–C(2)–C(19)	108.0
C(5)–C(6)	1.389	O(1)–C(2)–C(18)	104.1
C(6)–C(7)	1.386	C(3)–C(9)–C(19)	115.1
C(7)–C(8)	1.376	C(8)–C(2)–C(18)	109.9
		C(19)–C(2)–C(18)	110.8
		O(1)–C(9)–C(10)	125.2
		O(1)–C(9)–C(8)	114.2
		C(10)–C(9)–C(8)	120.5
		C(4)–C(10)–C(9)	120.8
		C(4)–C(10)–C(5)	121.4
		C(9)–C(10)–C(5)	117.8
		C(10)–C(5)–C(6)	121.9
		C(6)–C(7)–C(8)	120.7
		C(9)–C(8)–C(7)	119.6
		C(2)–O(1)–C(9)	117.5

[a] Estimated standard deviation of distances are 0.006–0.008 Å and of angles 0.4–0.7°.

and a listing of final structure factors are included as Supplementary Material.

The Dianin's compound xenon clathrate crystallizes in the trigonal space group $R\bar{3}$ with unit cell dimension a = 27.023(3) Å and c = 10.922 (1) Å. The calculated density for the hypothetical empty clathrate is 1.29 g cm^{-3}. The crystal and molecular structure of the parent Dianin's compound have been described in detail in several studies. A comparison of the geometry of the present compound with those previously reported show no significant differences. The observed bond distances and bond angles of the host molecules are very similar to a Dianin's compound clathrate with chloroform as the guest.[24] In essence the clathrate structure is formed by a hydrogen-bonded network involving the hydroxyl group of the host 4-*p*-hydroxyphenyl-2,2,4-trimethylchroman (**1**) molecules in rhombohedral symmetry with three molecules of one configuration pointing upwards and three of the opposite configuration pointing downwards (Figure 3). The oxygen atoms are grouped into hexagonal $[OH]_6$ rings. The space enclosed by the hexamer unit of the host molecules forms two half cavities. The shape of a single cage resembles an hourglass. The large voids centered at ca. 0.3 and 0.7 units along the crystallographic c axis have a van der Waals' diameter of 6.3 Å, whereas the "neck" of the hourglass at 0.5 is about 2.1 Å narrower. The van der Waals' radius of a xenon atom is about 2.20 Å and fits quite loosely in the cage. In principle each cavity can accommodate two xenon atoms. The separation between them will be 4.40 Å which corresponds closely to the minimum in the atomic xenon interaction curve.

In the xenon–Dianin's compound clathrate, the xenon position at (0,0,0.2850) and the symmetry related one (0,0,0.7150) are at the points of maximum extension in the cage. Refinement of the occupancy of xenon atoms indicated that approximately 71% of the cages were filled. The significant features in the final difference map were two peaks of 0.8 eÅ^{-3} near the xenon position. Therefore, it appears there is only one type of sorption site for the xenon in the clathrate from X-ray structure determination.

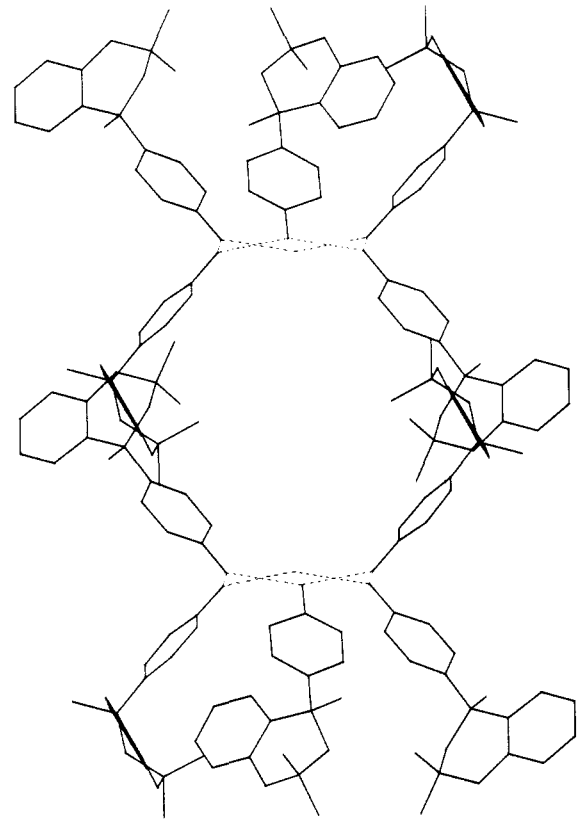

Figure 3. Stacking of the complex along the c axis. For clarity two host lattice molecules have been omitted.

Assignment of the ^{129}Xe NMR Spectrum. As the crystal structure determination shows only one type of absorption site, with the only other variable being the cage occupancies, the different ^{129}Xe lines must be interpreted in terms of small differences in local ordering due to the presence of empty or half-full cages. One way to test this hypothesis is to vary the number of filled Xe sites systematically. Early experiments were carried out by recrystallizing Dianin's compound from *m*-xylene under different Xe pressures. However, it was found that with low Xe pressure there was significant cage occupancy by the *m*-xylene solvent. A better solvent which was not taken up in the clathrate cages turned out to be dodecane.

Figure 4 shows ^{129}Xe spectra obtained for clathrate samples recrystallized from dodecane at xenon pressure between 0.3 and 10 atm of xenon. There are three kinds of cage configurations in this clathrate. Types 2 and 3 are shown in Figure 4, type 1 being the completely empty cage. On the basis of the spectra shown in the same figure, configuration 1 and 2 should predominate at low xenon contents, type 3 at high xenon content. Therefore, the high field xenon line should be assigned to configuration 2, and, as expected, it becomes less important as the xenon occupancy increases.

Since the two xenon atoms in one Dianin's compound cage lie ~4.40 Å apart, at a minimum in the Xe–Xe interaction potential, the Xe pair could be regarded as a Xe–Xe van der Waals' molecule. The 18 ppm chemical shift difference then represents a difference between the atom and the dimer. However, later on it will become evident that when the second xenon atom is replaced with ethanol, the shift remains nearly the same. It is not really clear whether the presence of a second guest in the cage is the primary reason for the shift, or whether the second guest causes a change in the configuration of the methyl groups at the neck of the cage, which in turn is sensed by the xenon atom.

The fine structure on the low field line, however, is still unexplained and is often not all that clearly defined for these samples. In order to produce more ordered crystals and, perhaps, better resolved spectra it was decided to produce samples with all cages filled but with different proportions of guests. The second

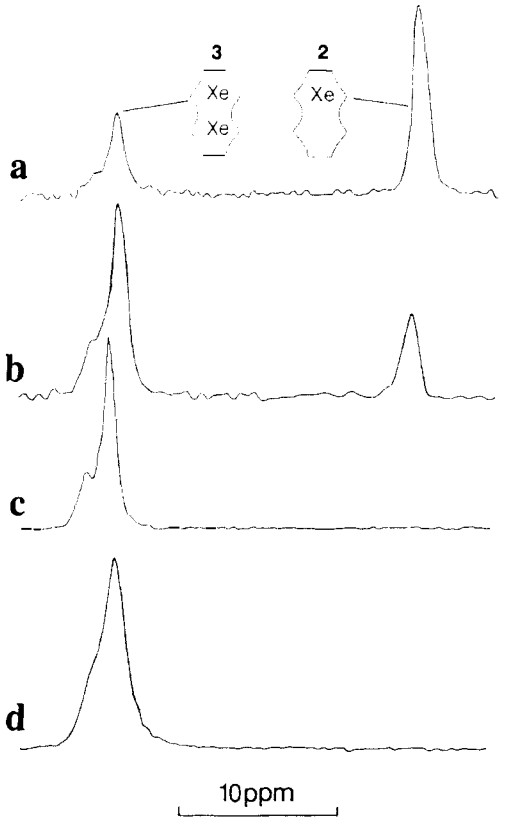

Figure 4. ^{129}Xe CP/MAS NMR spectra of Dianin's compound clathrates of xenon prepared from dodecane under different xenon pressures: (a) 0.3, (b) 0.7, (c) 3, (d) 20 atm.

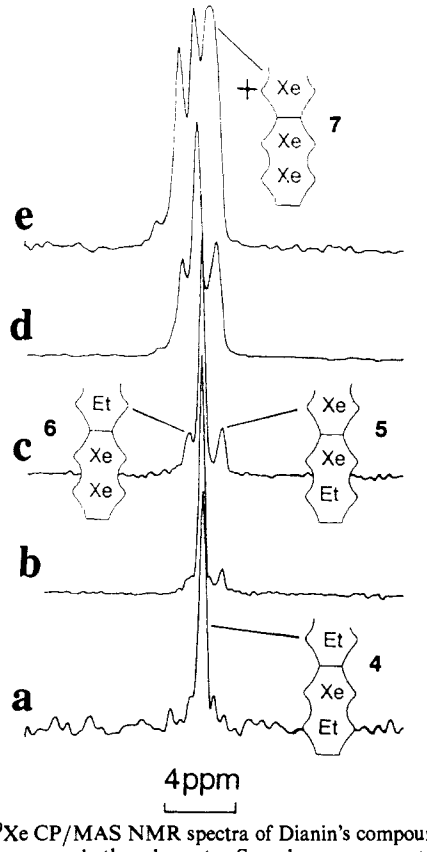

Figure 5. ^{129}Xe CP/MAS NMR spectra of Dianin's compound clathrate with mixed xenon and ethanol guests. Samples were recrystallized from ethanol under indicated xenon pressure: (a) 0.3, (b) 0.7, (c) 1.5, (d) 3, (e) 20 atm.

component of choice was ethanol, which is known to fit comfortably into one of the two wide portions of the cage.

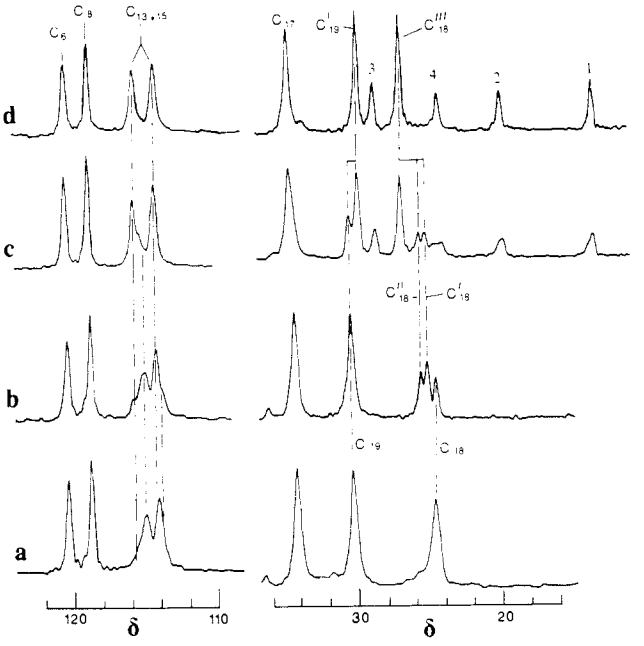

Figure 6. ^{13}C CP/MAS NMR spectra of Dianin's compound clathrates (a) empty, (b) sample recrystallized from dodecane under a low pressure of xenon, (c) sample recrystallized from octane under a low pressure xenon, (d) sample recrystallized from octane.

Figure 5 shows ^{129}Xe spectra of clathrate samples recrystallized from ethanol under different xenon pressures. First of all, the high field line was absent for all of these samples, in agreement with the absence of cage configuration 2. From the number of lines in some of the spectra, it appears that both nearest neighbors become important in determining the Xe nuclear shielding. The possible cage configuration for this set of samples then can be labeled 4–7. When Xe is very dilute, the only visible cage configuration should be no. 4, so that the relatively sharp line of Figure 5a can be assigned to this particular configuration. For completely random filling of cages, one may expect configurations 5 and 6 to be equally frequent, and Figure 5 (parts b and c) shows that two approximately equal intensity lines appear, flanking the main line to high and low field. With increasing pressure, the high field flanking line increases in intensity more rapidly than the low field line and this suggests that configuration 7 also occurs at the high field side.

The one feature which remains unexplained is the very weak low field shoulder which appears only for samples made under the highest xenon pressures. Also to be noted is the slight low field shift for all of the xenon lines as the xenon occupancy increases. Examination of static samples with differing xenon/ethanol occupancies shows only the powder pattern characteristic of the narrower shielding tensor in Figure 2c. This illustrates that indeed the site differences indicated in the spinning spectra are small. The NMR results are in accord with the X-ray picture, that is that only one type of site exists and that Xe resonance lines with different nuclear shielding are characteristic of differences in local ordering only. The xenon atom nuclear shielding is sensitive to the presence of a guest in the other half of the cage. The shielding difference is ~18 ppm and does not depend greatly on the nature of the guest. This fits the general observation that the isotropic Xe shifts in clathrate hydrates and clathrasils generally reflect the amount of free space in the clathrate cages irrespective of the type of host lattice material.

Assignment of the ^{13}C Spectrum. The information provided by the Xe spectrum can be used to advantage in assigning the ^{13}C NMR spectrum of the host lattice. For instance, a clathrate recrystallized from octane under a low pressure of xenon gives a rather complex spectrum, portions of which are shown in Figure 6c. The ^{129}Xe NMR spectrum for this sample as well as for a sample recrystallized from dodecane under a similar pressure of xenon is shown in Figure 7 (parts a and b). In both cases, cages

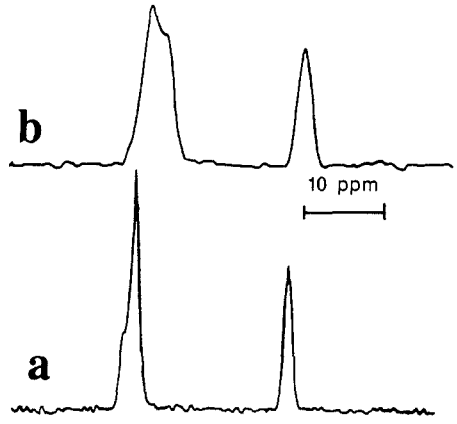

Figure 7. ^{129}Xe CP/MAS spectrum (a) same sample as described in Figure 6b, and (b) same sample as described in Figure 6c.

both singly and doubly occupied by xenon are indicated.

^{13}C NMR spectra for these two samples and for samples recrystallized from octane and dodecane (empty host lattice) are shown in Figure 6 (parts a–c). The C_{18} methyl carbon appears to be especially sensitive to the presence or absence of guest or to the nature of the guest. This is thought to originate in the flexiblity of the ring to which the C_{18} methyl is attached. The line marked C_{18} in Figure 6a corresponds to the empty host lattice. C_{18}' and C_{18}'' then correspond to cages filled or half-filled with xenon, and C_{18}''' corresponds to cages filled with octane. The C_{19} line also is sensitive to the presence of octane. This appears to be the general case for guests occupying the neck of the cage.

The lines due to C_{13} and C_{15} also show some sensitivity to the presence of guest molecules. The shift of these two carbons, being ortho to the phenolic hydroxyl group, is sensitive to the torsional angle of the OH group with respect to the plane of the aromatic ring. The torsional angle may well change depending on the cage content. Indeed, for the empty host lattice (Figure 6a) there appears to be some structure on the C_{13}, C_{15} lines and C_{18} as well. These features suggest the presence of some disorder in the empty lattice, related to rotation or movement of flexible parts of the host lattice molecules so as to partially occupy the empty cage space.

The lines due to enclathrated octane, labeled 1–4 in Figure 6d occur at 13.2, 19.4, 28.2, and 23.7 ppm. These positions are quite different from those measured in solution 13.9, 22.9, 32.2, and 29.5 ppm.[26] This can be explained by the fact that octane in the Dianin's compound cage is not in the extended all-trans configuration. X-ray diffraction has shown that the end methyl group of enclathrated *n*-heptanol, a molecule of similar length as octane, is gauche with respect to the C_4 methylene group. This conformer is considerably shorter than the all-trans form which cannot fit in the Dianin's compound cage. The same must be true for octane: rotation of the end methyl groups by 120° about the C_2–C_3 bond allows the incorporation of octane in the clathrate cage.

The presence of both xenon and octane as guests gives rise to a small shift in the octane carbon resonances, visible mainly as line broadening except for C_4 where two lines are partially resolved. Evidently the presence of two guests causes short-range disorder not only for the host lattice but also for guests in neighboring cages.

It is also clear from the ^{13}C and ^{129}Xe spectra that in no case is there evidence for clustering; i.e., cages with two Xe atoms per cage are not favored over cages containing a single Xe atom. One cannot expect exact statistical distributions of empty, half full, and completely full cages, as the samples were not prepared under equilibrium conditions.

Supplementary Material Available: Tables of atomic parameters and anisotropic temperature factors and a conversion chart of the numbering for Dianin's compound atoms (3 pages); table of observed and calculated structure factors (17 pages). Ordering information is given on any current masthead page.

Separation by ^{23}Na NMR of the Unimolecular and Bimolecular Components of the Dissociation Kinetics of 18-Crown-6-Na^+ in Some Nonaqueous Solvents

Helen P. Graves and Christian Detellier*

Contribution from the Ottawa-Carleton Chemistry Institute, Ottawa University Campus, Ottawa, Ontario K1N 9B4, Canada. *Received December 29, 1987*

Abstract: The kinetics of dissociation of (18-crown-6, Na^+)[1] in propylene carbonate (PC), acetonitrile (AN), pyridine (PY), and acetone (AC) have been determined by ^{23}Na NMR. Two mechanisms of exchange, namely unimolecular dissociative and bimolecular, have been shown to be in competition in the first three solvents. In acetone, the exchange mechanism is almost exclusively unimolecular. The activation parameters for the unimolecular exchange have been determined in all four solvents. $\Delta H^{\ddagger}_{uni}$ follows the trend AN < AC < PY $\simeq$ PC. A compensation effect between $\Delta H^{\ddagger}$ and $\Delta S^{\ddagger}$ was observed. As a result, $\Delta G^{\ddagger}_{300K}$ is in the range 50–58 kJ·mol^{-1} (AC and PY, respectively). No direct relationship between the Gutmann donicity number and $\Delta G^{\ddagger}$ or $\Delta H^{\ddagger}$ could be established, showing that several factors, including conformational rearrangement of the ligand and reorganization of the solvent cage, contribute to the barrier of exchange. The activation parameters were also determined for the bimolecular exchange mechanism in PC: $\Delta H^{\ddagger}_{bi} = 35 \pm 1$ kJ·mol^{-1} and $\Delta S^{\ddagger}_{bi} = -16 \pm 3$ J·K^{-1}·mol^{-1}.

The recognition of cations by macrocyclic hosts is well documented.[2] However, the factors responsible for the recognition are far from being well understood, particularly the role of the solvent. There are only a few studies in the literature which deal with the kinetics of the crown ether–alkali metal cation association/dissociation processes.[3-15] Since the rate of formation of

(1) 18-Crown-6 (18C6): 1,4,7,10,13,16-hexaoxacyclooctadecane.

(2) (a) Sutherland, I. O. *J. Chem. Soc., Faraday Trans. 1* **1986**, *82*, 1145–1159. (b) Lehn, J-M. Science (*Washington, D.C.*) **1985**, *227*, 849–856. (c) Takeda, Y. In *Host–Guest Complex Chemistry III*; Vögtle, F., Weber, E., Eds:; 1984; Vol. 121, pp 1–38. (d) Hilgenfeld, R.; Saenger, W. In *Host–Guest Complex Chemistry II*; Vögtle, F., Ed.; 1982; Vol. 101, pp 1–82. (e) *Host–Guest Complex Chemistry I*; Vögtle, F., Ed.; 1981; Vol. 98.

(3) (a) Shchori, E.; Jagur-Grodzinski, J.; Luz, Z.; Shporer, M. *J. Am. Chem. Soc.* **1971**, *93*, 7133–7138. (b) Shchori, E.; Jagur-Grodzinski, J.; Shporer, M. *J. Am. Chem. Soc.* **1973**, *95*, 3842–3846.

(4) Shporer, M.; Luz, Z. *J. Am. Chem. Soc.* **1975**, *97*, 665–666.

(5) (a) Mei, E.; Popov, A. I.; Dye, J. L. *J. Phys. Chem.* **1977**, *81*, 1677–1681. (b) Mei, E.; Dye, J. L.; Popov, A. I. *J. Am. Chem. Soc.* **1977**, *99*, 5308–5311.

0002-7863/88/1510-6019$01.50/0 © 1988 American Chemical Society